Column Study for Assessing the Influence of Soil Compaction on CH$_4$ Oxidation in Landfill Covers

Final Report

February 2009

Dr. Julia Gebert, Ingke Rachor & Dr. Alexander Gröngröft

University of Hamburg
Institute of Soil Science
Allende-Platz 2
D-20146 Hamburg

Tel. ++49 40 42838 6595
Fax. ++49 40 42838 2024
j.gebert@ifb.uni-hamburg.de

Table of contents

List of figures

List of tables

1 Background and study aims

The microbial oxidation of methane in engineered cover soils is considered a potent option for the mitigation of low calorific emissions from landfills. The oxidation efficiency is regulated by the combination of cover material properties, landfill gas source strength and climate conditions. Under given climatic conditions and methane production rates, especially the physical properties of the soil are of eminent importance. Soil texture and compaction determine the pore size distribution effective for both water retention and gaseous transport, thus determining the rate at which methane and atmospheric oxygen become available to the methane oxidising microorganisms. In order to derive design criteria that enable composing an effective methane oxidising cover layer from the range of soils that become available to the landfill operator, a laboratory column study was conducted to assess the methane oxidation capacity of a soil at different degrees of compaction under simulated landfill conditions. In addition, aliquots of the soil material were used in a separate experiment to measure soil gas diffusivity at the corresponding degrees of compaction.

The column study was carried out by the University of Hamburg, Institute of Soil Science, as a subcontractor of melchior+wittpohl Ingenieurgesellschaft Hamburg. The contract included the sampling of soil on Nauerna landfill, the technical setup in the laboratory, the filling of columns with the soil material, column operation, diffusivity testing, data collection, data analysis and interpretation. Soil physical analyses were carried out by melchior+wittpohl Ingenieurgesellschaft.

2 Collection and characterisation of Nauerna landfill cover soil

The soil was collected on July 2, 2008. A trench of approximately 1 m width was excavated in parallel to the slope by Nauerna landfill staff (Figure 2). Soil was collected from one location each on the upper, the middle and the lower section of the slope (Figures 3 to 5). At these locations, undisturbed samples were taken for bulk density analysis from two depths using two steel cylinders per depth (diameter 10 cm, height 12 cm).

Figure 1: Sampling area.

Figure 2:   Excavation of trench.

Figure 3:   Soil profile at the upper slope.

Figure 4: Soil profile at midslope.

Figure 5: Soil profile at the lower slope.

As all three soil profiles were very similar, a general description is given concerning the features that were observed on site. Classifications according to the Bodenkundliche Kartieranleitung (Ad-Hoc-Arbeitsgruppe Boden 2005) are printed in italics.

In all three positions the soil was very compacted (bulk density class *LD 4-5*). Only in the upper 20 cm, the bulk density was partly lowered to *LD 2* as a result of the plant root penetration (*LD 2+4*; *W5* = 21-50 roots/dm^2). As a result of rooting and evapotransporation-mediated desiccation of the soil, the upper 20 cm were aggregated (soil structure types: subangular, *sub*, and platy, *pla*). Below 20 cm, the soil was not aggregated but classified as coherent, *koh*. Consis-

tently, the number of roots also decreased sharply below this depth (W1 to W0 = 0-2 roots/dm^2). As a result of the high compaction and the subsequent low degree of aeration, hydromorphic features were clearly visible across the entire depth of all profiles. Grey patches signify areas discoloured under reducing conditions, usually depleted in iron and manganese, whereas orange patches signify precipitation of iron oxides under oxidising conditions (Figure 6).

Mussel shells were found in all profiles.

Figure 6: Hydromorphic features in the midslope profile.

According to the texture analysis (sieving and sedimentation according to DIN 18123), the bulk soil (fraction < 2 mm) consisted of 14.0 % clay, 20.3 % silt and 64.8 % sand and was classified as *stark lehmiger Sand* according to Bodenkundliche Kartieranleitung. According to the World Reference Base (FAO 2006), the soil would be classified as a sandy loam. Figure 7 shows the water retention curves determined for the three degrees of compaction, the corresponding key properties are listed in Table 1. The data clearly indicate that the compaction most affects the share of pores > 50 µm, also referred to as air capacity, which are always drained and thus are available for gas transport. The degree of compaction thus greatly influences the transport of oxygen into soils and can thus be expected to significantly influence CH$_4$ oxidation rates. Also, compaction increases the share of pores < 0.2 µm, which do not contribute to the plant-available water. Compaction therefore not only reduces the air capacity but also the available field capacity.

Throughout this report, the three columns are labelled column 1 (compaction to 95 % of the Proctor density), column 3 (85 %) and column 4 (75 %). The numbering 1, 3 and 4 (with '2' missing) results from the according labelling of the laboratory equipment.

Table 1: Characteristic parameters derived from the water retention curve. Field capacity and air capacity were assigned to the matric potential of 60 hPa.

Parameter	Column 1	Column 3	Column 4
Compaction [% Proctor]	95	85	75
Total pore volume [vol.%]	41.08	47.57	54.28
Air capacity [vol.%]	2.30	8.13	19.08
Field capacity [vol.%]	38.78	39.43	35.20
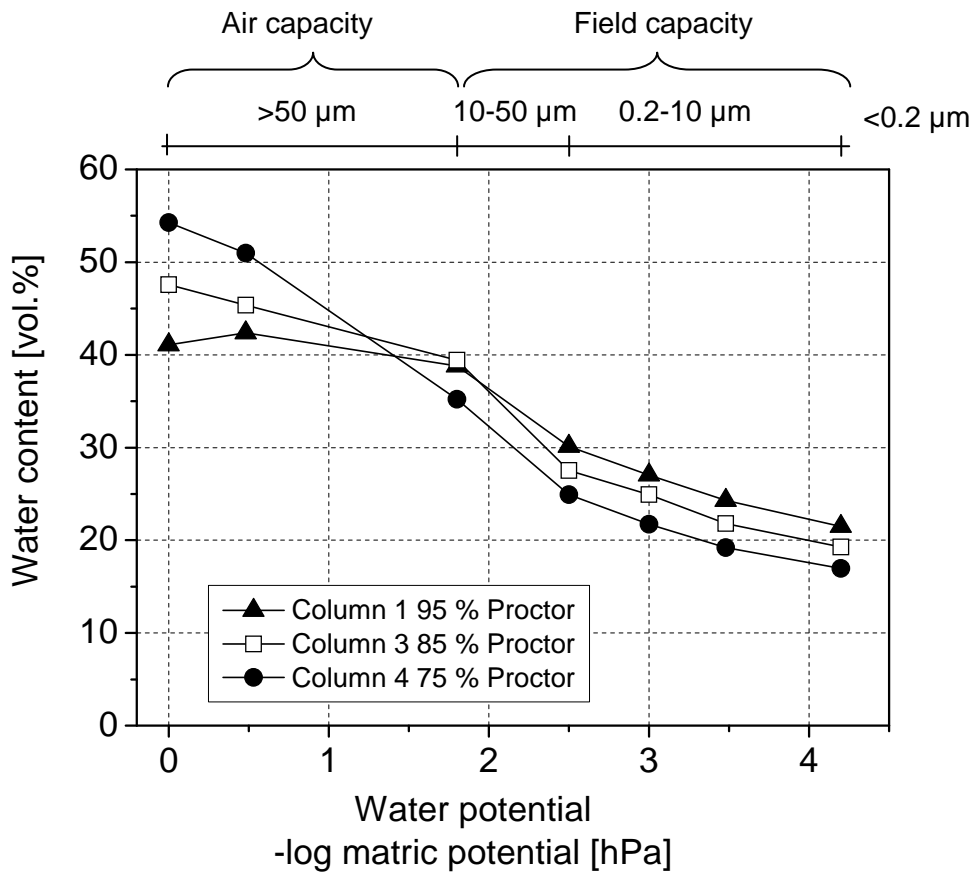
Figure 7: Water retention curves for the three degrees of compaction. Each symbol represents the average of 5 samples. Water potential is given as –log ψ_m [hPa], where ψ_m is the matric potential of the material. Top of figure: corresponding pore diameters.

The data points for the water retention curves shown in Figure 7 are based on the determination of the total pore volume by pycnometry. melchior+wittpohl Ingenieurgesellschaft used a different methodological approach and calculated the total pore volume assuming a standard particle density. As a result, the final retention curves presented in the two reports can deviate from eachother.

Column setup

Three columns where constructed from PVC-pipes (DIN EN 1401-1) with a length of 1070 mm, an inner diameter of 190 mm and a wall thickness of 4.9 mm. They were closed with sealing caps at both ends. At the bottom, an inlet for synthetical landfill gas and at the top an inlet for (synthetical) air and a clean gas outlet were installed. Vertically, gas sampling points were mounted in 10 cm intervals, consisting of a needle penetrating a tightly sealed butyl-rubber stopper and reaching 10 cm into the substrate. The needles where closed with a disposable 1 ml syringe used for sampling the soil gas. At the bottom, a water outlet was installed to provide a drainage in case of leachate build-up. For security reasons the entire setup was placed under a fume hood. The temperature was monitored using a Pt100 temperature sensor placed in the fume hood.

Each column was packed with a gas distribution layer of 17 cm of coarse gravel, topped by 80 cm of soil. Before, the soil water content was adjusted to the average water content at 60-300 hPa suction for the given texture according to Table 75 of Bodenkundliche Kartieranleitung (Ad-Hoc-Arbeitsgruppe Boden 2005). The soil was compacted to 75 %, 85 % and 95 % of the Proctor density. Soil physical properties are shown in Table 2. Installation and compaction of the soil was performed in 10 cm intervals. Interface effects between layers were minimized by scraping off the top cm of each layer before placement and compaction of the subsequent layer. A scheme of the setup can be seen in Figure 8. Inlet and outlet flow rates were controlled with needle valves and recorded using rotameters operating in the range of 0-19 ml/min (inlet) and 0-150 ml/min (outlet), at a total height of 150 mm each (purchased from ANALYT-MTC Messtechnik GmbH).
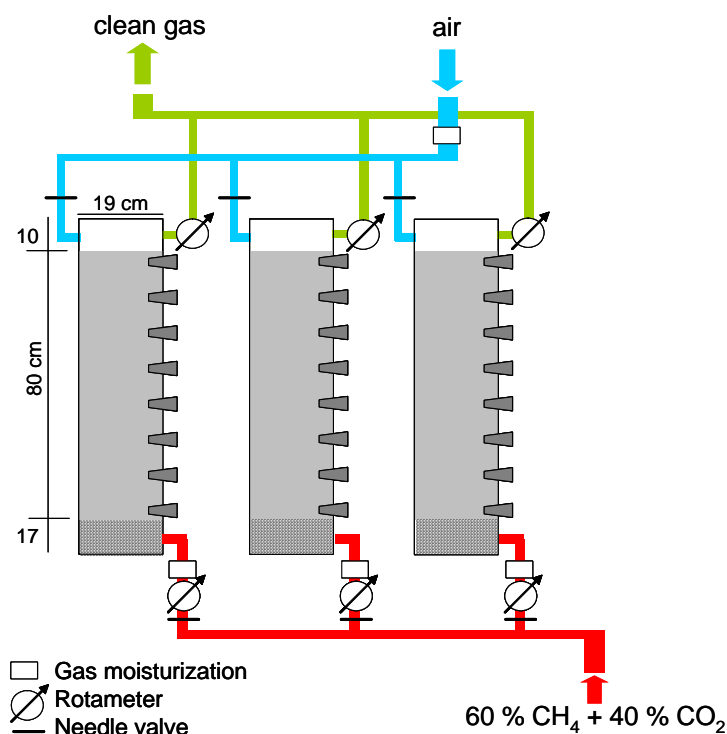
Figure 8: Schematic of column setup, not to scale.

Table 2: Dimensions of columns; water content, solids and pore volumes, air capacity and water content of column materials (not considering the gas distribution layer). ww = wet weight, dw = dry weight.

Inner diameter [cm]	19		
Base area [m²]	0.02835		
Column no.	**1**	**3**	**4**
Height (incl. gravel) [cm]	97	97	97
Height (soil) [cm]	80	80	80
Weight (soil) [kg ww]	41.34	36.99	32.64
Bulk density [g dw/cm³]	1.59	1.42	1.25
Water content [kg]	5.75	5.15	4.54
Solids volume [l]	13.43	12.02	10.60
Pore volume in [l]	9.0	10.42	11.83
Pore volume [vol. %]	40.13	46.43	52.74
Water content [vol. %]	25.65	22.95	20.25
Gas volume [vol. %]	14.48	23.48	32.49

If comparing the values for the water content given in Table 2 with the water retention curves shown in Figure 7, it can be noted that the final water contents were lower than those corresponding to the average value of 60 and 300 hPa. This is due to the fact that the Bodenkundliche Kartieranleitung only provides rough estimates that cannot cover texture details, for example, considering the nature of the sand fraction (fine, middle or coarse sand).

3 Experimental procedures

The columns were continuously charged with synthetical landfill gas (40 vol.% CO$_2$, 60 vol.% CH$_4$) derived from a pressurized bottle connected to the gas distribution system (red piping in Figure 8). The gas was passed through a water bottle before entering the columns in order to prevent desiccation of the soil. Flow rates were controlled with needle valves and the inlet rotameter valves. At the top, moisturized air was pumped through the column headspaces at an excess rate compared to the inlet flux. Headspace flux was controlled by needle valves positioned before the air inlet. Total effluent (outlet) gas flux was displayed by rotameters located behind the gas outlet. The flow rates for synthetical landfill gas were run within three different test ranges (Table 3).

Table 3: Phases of column operation. Std. dev. = standard deviation.

Phase no.	Date	Inlet CH$_4$ flux [l m^{-2} h^{-1}]	Std. dev.
1	21.08.-24.09.08	2.24	0.42
2	25.09.-15.10.08	3.58	0.76
Construction works in laboratory, no operation			
3	24.11.-04.12.08	5.27	0.59

3.1 Gas profiles

The vertical distribution of CH$_4$, CO$_2$, O$_2$ and N$_2$ within the individual columns was determined weekly for nine depths per column using a GC-FID/TCD (Agilent). 1 ml of sample was withdrawn from the respective depth and directly analysed.

3.2 Calculation of CH$_4$ oxidation efficiency

Inlet and outlet fluxes were recorded five times per week and combined with the analysis of CH$_4$- and CO$_2$-concentrations in the headspace using a GC-FID/TCD (Shimadzu 14A/B) to calculate CH$_4$ and CO$_2$ inlet and outlet fluxes. CH$_4$ oxidation efficiency was calculated as follows:

$$CH_4 ox = \frac{(flux_{in} - flux_{out})}{flux_{in}} \times 100 \qquad \text{Eq. 1}$$

where $CH_4 ox_{\_i}$ = % of CH$_4$ inlet flux oxidized at time i

          $flux_{in\_i}$ = CH$_4$ flux into the column (ml/min) at time i

          $flux_{out\_i}$ = CH$_4$ flux out of the column (ml/min) at time i.

To account for the (residence) time lag between inlet and corresponding outlet fluxes, outlet fluxes were related to inlet fluxes calculated as a moving three day average.

3.3   Diffusion tests

Aliquots of the Nauerna cover soil were packed into triplicate 100 cm^3 steel soil cores at 75 %, 85 % and 95 % of the Proctor density. The share of air-filled pore volume was determined by pycnometry and the soil cores then placed in a diffusion chamber which was purged with N$_2$ (Figure 9a). Diffusive re-entry of atmospheric O$_2$ into the chamber via the soil core was monitored by GC-TCD analysis (Figure 9b).

By means of simple box modelling, the obtained effective diffusion coefficients were used to simulate the ingress of O$_2$ against a prevailing advective landfill gas flux.
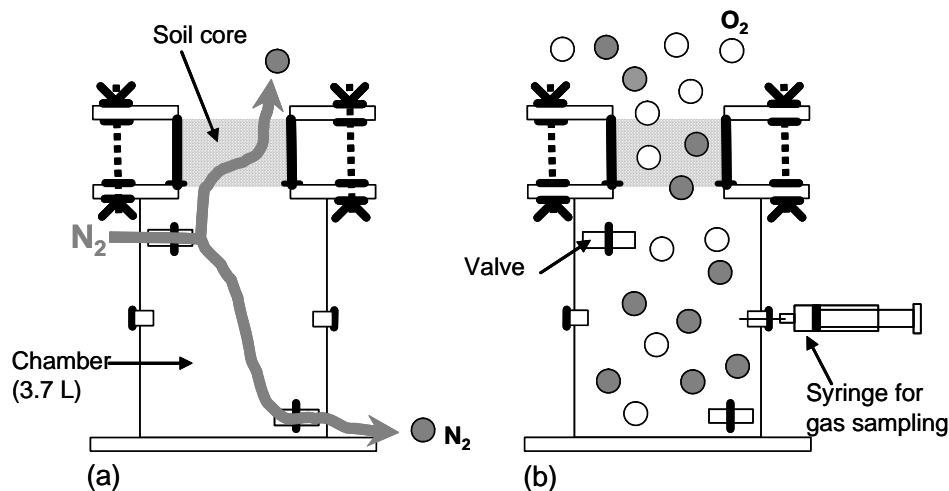
Figure 9:   Setup of diffusion test, not to scale.

3.4   Quality management

The following measures were taken to ensure quality of column operation, GC measurements and data processing:

- All junctions and interfaces where sealed and tested for gas-tightness before and in the course of the experiment by means of a portable FID.
- In a separate experiment it was verified that the disposable syringe and needle setup used to collect gas profile samples did not provide a pathway for diffusive influx of air into the columns.
- Inlet and outlet fluxes were controlled daily and adjusted if necessary.
- The Shimadzu GC-FID/TCD was calibrated daily for CH$_4$ and CO$_2$ using 7 standard gas mixtures.
- Stability of the Agilent GC-FID/TCD calibration for CH$_4$, CO$_2$, O$_2$, and N$_2$ was checked regularly using 3 standard gas mixtures.
- Rotameter calibration supplied by the producer was corrected by triplicate soap film flow meter measurements covering the entire range of flow rates applied.

3.5   Potential for errors

As the clean gas was lead off from the laboratory to the outside atmosphere, outlet rotameter readings sometimes oscillated strongly under windy weather conditions. In these cases, the average flow rate of the range over which the flow oscillated was selected for outlet CH$_4$ flux calculations. Calculated CH$_4$ outlet fluxes could be lower or higher than the actual value.

4 Results of column study

4.1 Soil diffusivity

Figure 10 shows that in the given material soil diffusivity, signified by the effective diffusion co-efficient, depended strongly on the degree of compaction and thus on the pore volume available for gas transport. D$_{eff}$ varied by a factor of 5.7 between samples compacted to 95 % and samples compacted to 75 % of the Proctor density. The water contents of the material correspond to a matric potential of approximately 300 hPa.
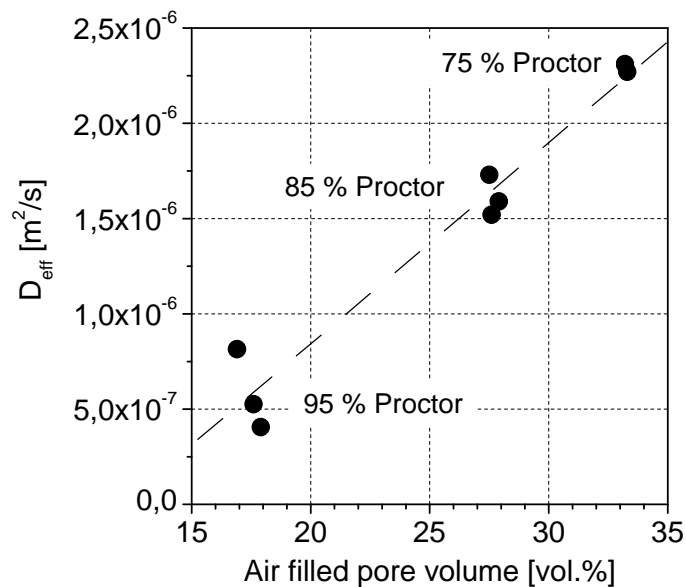

Figure 10: Relationship between the share of air-filled pore volume and soil gas diffusivity.
       D$_{eff}$ = effective diffusion coefficient.

Table 4: Effective diffusion coefficient for different degrees of compaction at a matric potential around 300 hPa.

	Average D$_{eff}$ [m^2/s]
75 % Proctor	2.29*10^{-6}
85 % Proctor	1.61*10^{-6}
95 % Proctor	5.82*10^{-7}

4.2 CH$_4$ oxidation efficiency

The columns were exposed to synthetical landfill gas and air for a week before measurements were started to allow for system equilibration and activation of the methanotrophic community. When monitoring started, oxidation could be observed immediately in all columns (Figure 11). Methane reduction took part in all three columns during the entire period of the experiment. However, the performance at the different degrees of compaction varied strongly , both for the same substrate over time and as a result of changing inlet CH$_4$ fluxes, as well as between columns.
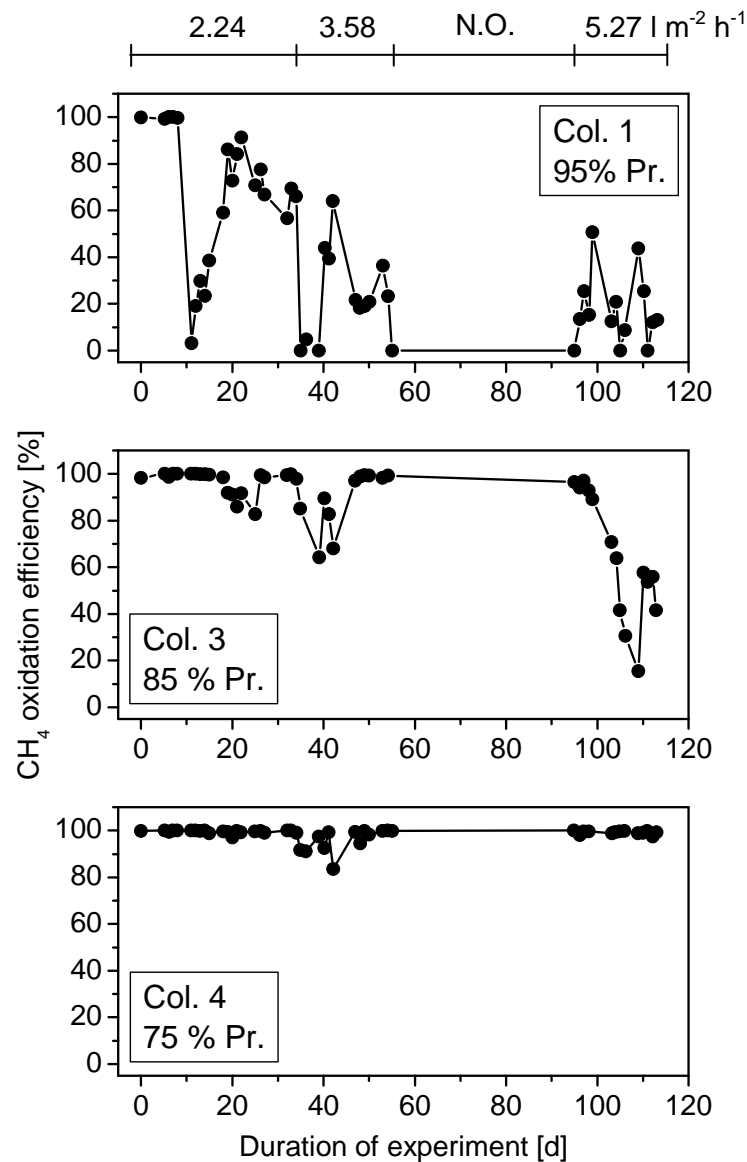
Figure 11: CH$_4$ oxidation efficiency in the course of the column experiment. Top of figure: indication of inlet fluxes during the three operational phases (compare Table 3). N.O. = no operation (construction works in laboratory).

Column 4 (75 % Proctor density) maintained an oxidation efficiency of close to 100 %, regardless of the magnitude of the inlet flux. Columns 1 and 3 reacted more sensitively to the increase in inlet flux. After a sharp decrease in oxidation efficiency with the two increases in flux, column 3 (85 % Proctor) regained a high efficiency within a few days, whereas column 1 (95 % Proctor) only recovered to a poor average performance of 22 % and 17 %, respectively. Methane oxidation efficiencies at the different loading rates are clarified in Figure 12.
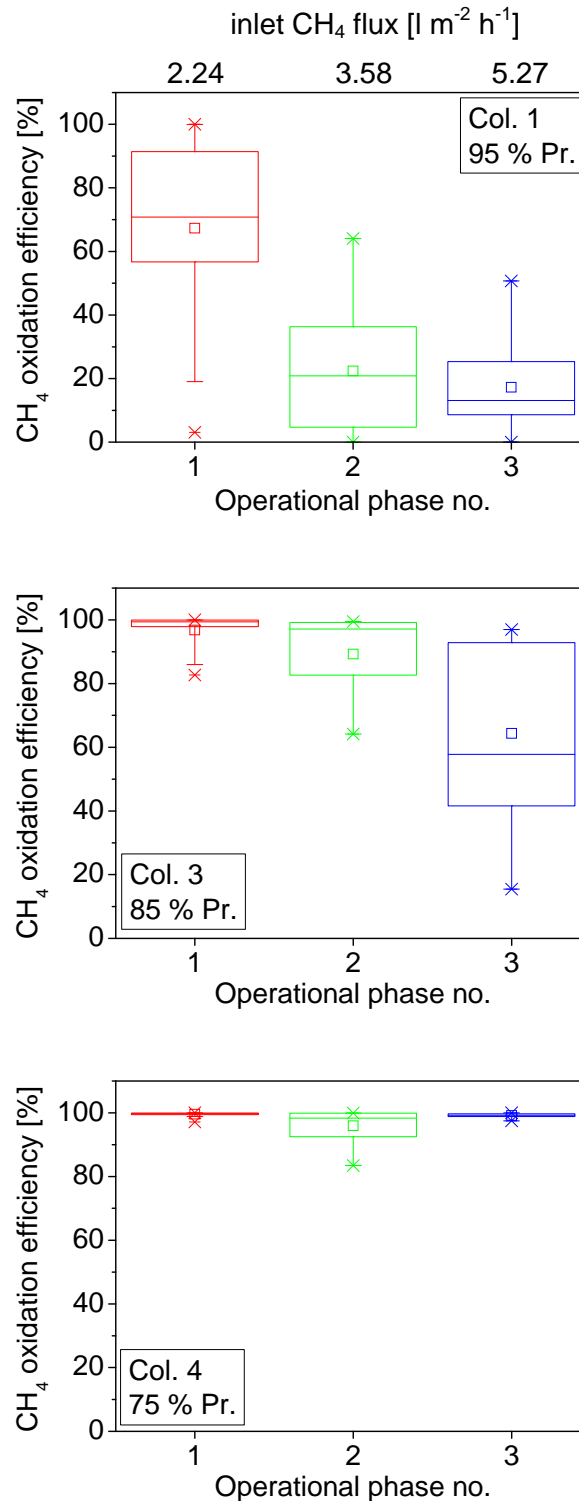
Figure 12: CH₄ oxidation efficiency for all columns during the three operational phases. Box = values within the 25th and the 75th percentile, line = median, symbol = artithmetic mean, whisker = values within the 5th and the 95th percentile, crosses = values between the 1st and the 99th percentile, short horizontal lines = maximum and minimum.

Performance of columns 1 and 3 decreased with increasing inlet fluxes (phases 1 to 3), whereas the capacity limit of column 4 was not reached during the experiment. Whereas performance plummeted in the 95 % Proctor column after a flux increase to 3.58 l m^{-2} h^{-1}, oxidation

performance in the 85 % Proctor column only decreased after a flux increase to 5.27 l m^{-2} h^{-1}, however, still maintaining an average of > 60 % efficiency. The high variability in column 3 efficiency at the high loading rate indicates the sensitivity of the system at loading rates around the capacity limit of the column. A factor possibly affecting system performance at high loading rates is the humidity of the sweep air in the column headspace and subsequently the water content of the upper soil crust.

4.3   CH$_4$ oxidation at different inlet fluxes

The relationship between inlet CH$_4$ fluxes and the absolute CH$_4$ degradation rates for all measured values is shown in Figure 13. To facilitate estimation of the percentage oxidation efficiency, the graphs include the 100 % oxidation rate as straight line.
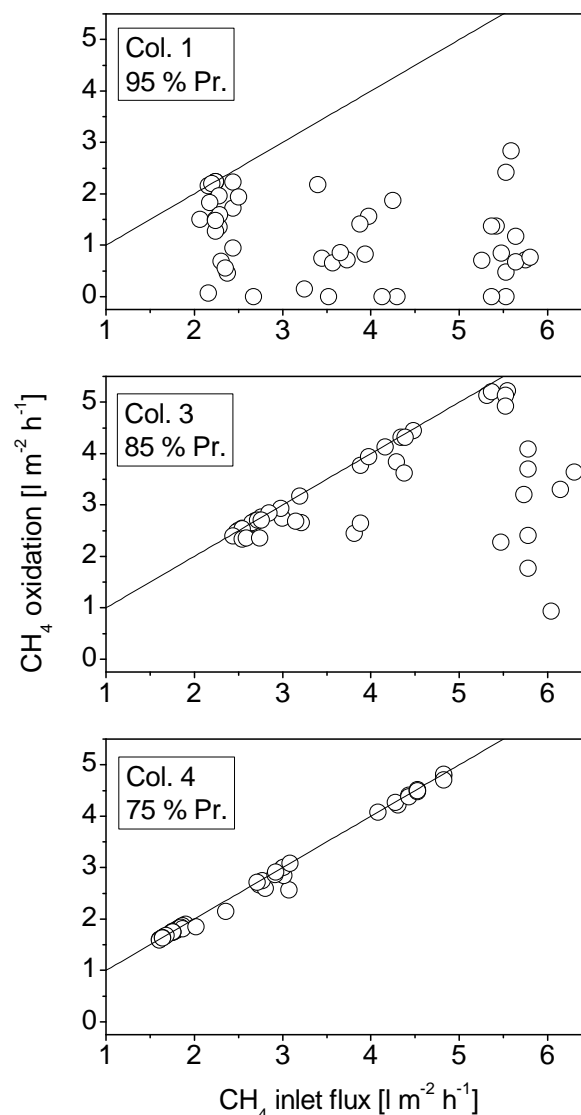

Figure 13: Absolute CH$_4$ oxidation rates as a function of inlet CH$_4$ flux. Black line: x=y (100 % oxidation efficiency). Red line = estimated column oxidation capacity curve.

Columns 3 and 4 columns show increasing absolute removal rates with increasing influx rates. CH$_4$ oxidation rates by column 1 usually were well below the applied CH$_4$ loading rates. It has

to be noted, and this applies to the previous figures as well, that the loading rate of column 4 was always a bit lower than that of the other columns. This was due to individual specifications of the rotameters, which read slightly different fluxes for identical graduations.

4.4 Gas profiles

The vertical distribution of CH$_4$, CO$_2$, O$_2$ and N$_2$ was analysed weekly in order to derive the extent of the ingress of atmospheric air and thus to localize the depth of the active CH$_4$ oxidation horizon. As O$_2$ is consumed by both CH$_4$ oxidation and heterotrophic respiration, N$_2$ was used for the assessment of the ingress of air.

For each column, Figure 14 to Figure 16 show selected gas profiles that are representative for each operational phase.
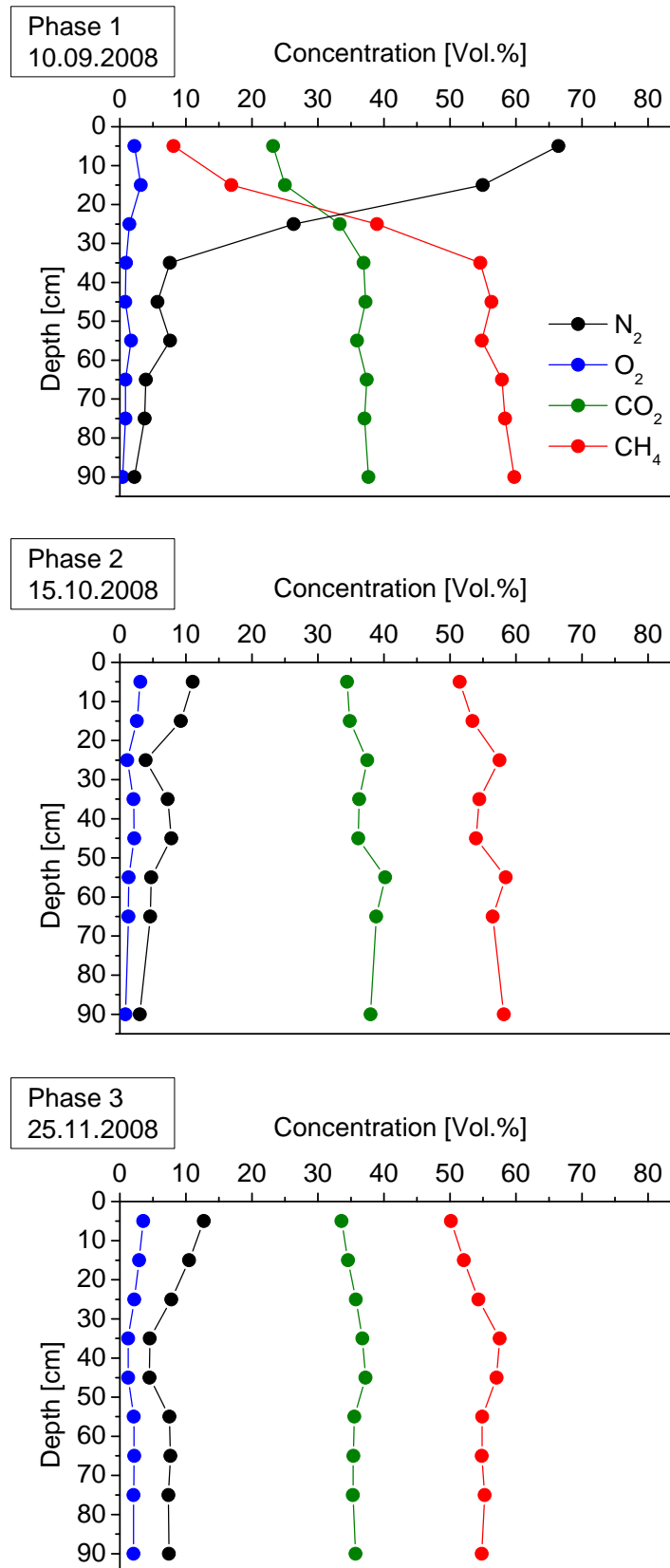
Column 1 (95 % Proctor)

Figure 14: Column 1 gas profiles for the three operational phases.
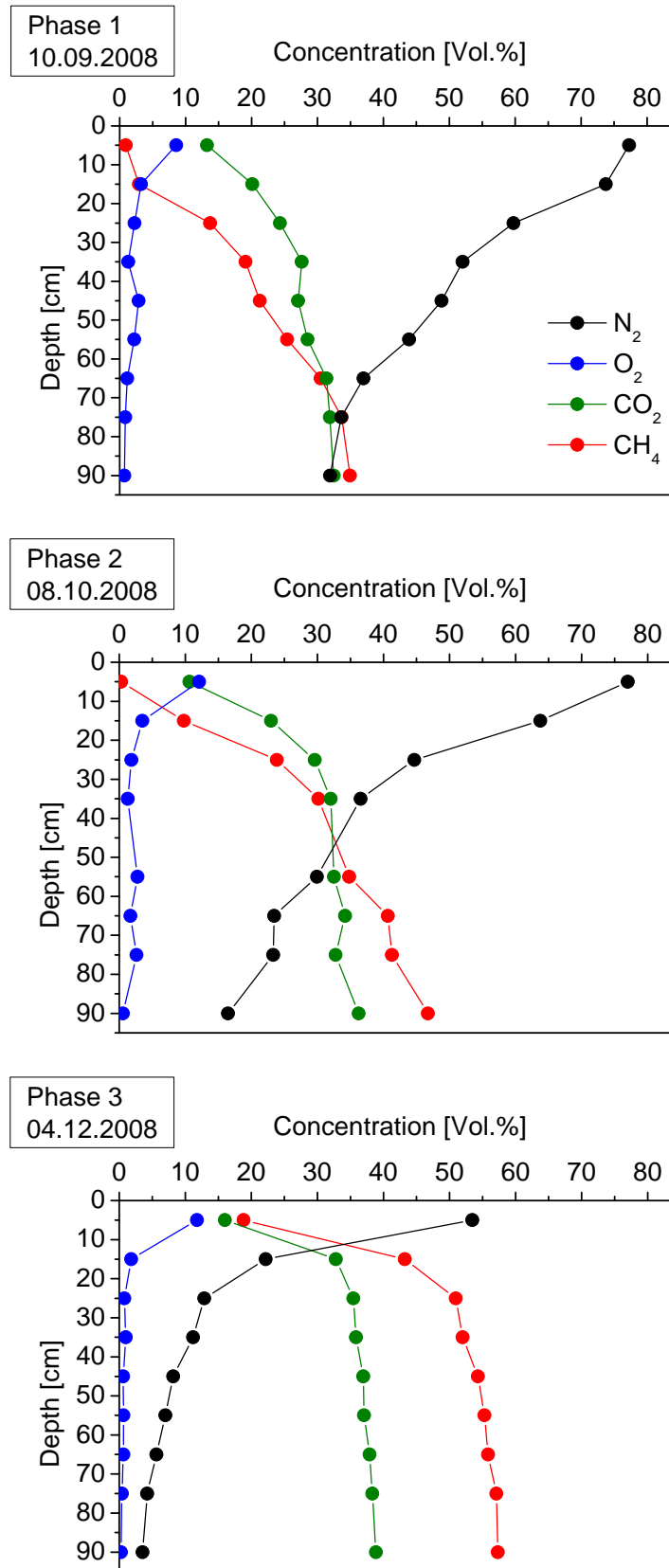
Column 3 (85 % Proctor)

Figure 15: Column 3 gas profiles for the three operational phases.

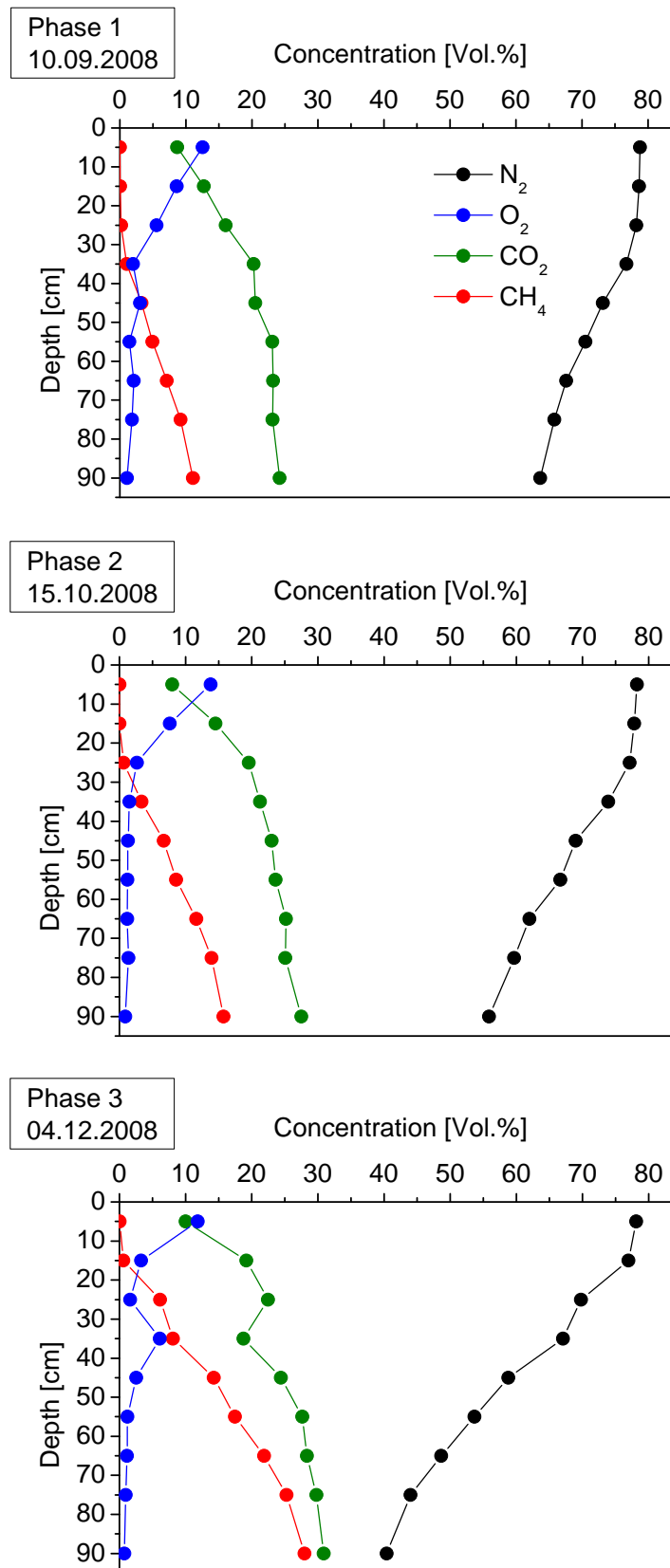**Column 4 (75 % Proctor)**

Figure 16: Column 4 gas profiles for the three operational phases. 90 cm depth = gravel layer.

As expected, the gas profiles show that the diffusive ingress of air increases with decreasing bulk density and with increasing advective bottom flux. In column 1 (95 % Proctor), diffusive ingress of atmospheric air only reached significant levels in phase 1, i.e. at the lowest bottom flux. As indicated by the concentration of N$_2$, the top 35 cm of the column were aerated and served as CH$_4$ oxidation horizon. This is confirmed by the increasing CO$_2$-CH$_4$ ratio in the soil gas phase from 35 cm depth towards the top (Table 5). Increased fluxes in phase 2 and 3 resulted in a strong decline of the extent of aeration already within the top decimetre. As in the previous column study (see Gebert et al. 2008), CH$_4$ oxidation was restricted to the upper few centimetres of the column. This is confirmed by the CO$_2$-CH$_4$ ratio which did not change up to 5 cm depth.

At a bulk density of 85 % of the Proctor density, aeration was greatly improved. During phase 1 and 2, the column was well aerated down to the base, even into the gas distribution layer (gravel). The continuous increase in the CO$_2$-CH$_4$ ratio from bottom to top indicates that the microbial CH$_4$ oxidation occurred across the entire length of the column. Increase of the bottom flux level to 5 l m^{-2} h^{-1} significantly decreased the ingress of air, but an oxidation horizon of 45 cm was still maintained. The ratio of CO$_2$ to CH$_4$ increased from 45 cm towards the top but not significantly until a depth of 15 cm, indicating that under these flux conditions a reduced oxidation horizon was established.

At very low compaction (column 4, 75 % Proctor density), the entire column was well aerated across the entire range of bottom fluxes tested. Nevertheless, Figure 16 shows that in this column also increasing fluxes reduced the extent of atmospheric N$_2$ penetration. Strongly elevated CO$_2$-CH$_4$ ratios in the gravel layer of 1 to > 2, compared to the CO$_2$-CH$_4$ ratio of the feed gas (0.67), indicate that as a result of the good aeration CH$_4$ oxidation already occurred in the gravel layer.

Table 5: Ratios of CO$_2$ to CH$_4$ in the different depths for the gas profiles shown in Figure 14, Figure 15 and Figure 16.

Depth [cm]	Column 1 (95 % Pr.)			Column 3 (85 % Pr.)			Column 4 (75 % Pr.)		
	Phase 1	Phase 2	Phase 3	Phase 1	Phase 2	Phase 3	Phase 1	Phase 2	Phase 3
5	2.85	0.67	0.67	14.22	34.80	0.85	727.55	13204.86	193.00
15	1.48	0.66	0.65	6.93	2.35	0.76	358.68	3177.72	32.78
25	0.86	0.66	0.65	1.77	1.24	0.70	82.54	30.88	3.66
35	0.68	0.64	0.67	1.45	1.06	0.69	19.60	6.37	2.32
45	0.66	0.65	0.67	1.27	0.97	0.68	6.30	3.43	1.71
55	0.66	0.65	0.69	1.12	0.93	0.67	4.68	2.76	1.58
65	0.65	0.65	0.66	1.03	0.84	0.68	3.27	2.17	1.30
75	0.64	0.64	0.70	0.95	0.79	0.67	2.51	1.80	1.18
90	0.63	0.65	0.65	0.93	0.78	0.68	2.18	1.75	1.10

4.5 Limits on microbial CH$_4$ oxidation induced by low diffusivity – a worst case scenario

In order to assess the importance of compaction and thus of construction practice, simple calculations were performed to estimate the flux of CH$_4$ that can be oxidised in a 'worst case' scenario of compaction to 95 % of the Proctor density. The following assumptions were made:

- Air-filled pore volume under very well drained conditions (matric potential = 300 hPa) = 10.96 Vol.% (compare Figure 7).

- From our dataset of correlation between air-filled pore volume and diffusivity, the following equation, derived from a linear regression (n = 40, R^2 = 0.92) was applied:

  D_{eff} = 7*10^{-8} × pore volume - 7*10^{-7}; D_{eff} in m^2/s, pore volume in vol.%

  The dataset includes the samples presented in Figure 10.

- According to the nominal CH$_4$ oxidation reaction equation O$_2$ flux into the 'active layer' of methane oxidation must be double that of the CH$_4$ flux charged to the active layer. O$_2$ influx must be twice as much as landfill gas efflux to ensure ingress of the required O$_2$ quantity.

- Height of the active layer was varied between 0.05 and 0.4 m. The concentration of O$_2$ at the base of the active layer is zero, at the top it is 21 vol.%.

- Landfill gas composition is 60 % CH$_4$ and 40 % CO$_2$.

Table 6 shows the results for different heights of the active CH$_4$ oxidising layer. The maximum acceptable landfill gas flux to the cover increases with decreasing depth of the active layer as a result of the steeper O$_2$ concentration gradient and thereby increased O$_2$ flux. The 'upper limit' to this approach is given by the CH$_4$ oxidation potential of soil. The last column of Table 6 shows which activity the maximum CH$_4$ fluxes correspond to, if all CH$_4$ would be oxidized. The values are well within the data presented in the literature. Maximum activity in the 10 cm cover soil on a methane oxidising biofilter was measured to be 10 µg g^{-1} h^{-1} (Gebert et al. 2003). However, these data were obtained at 22 °C incubation temperature. Assuming an annual average of only 10 °C in the top decimetre of a soil under ambient climatic conditions, the average activity will not be higher than approximately 5 µg g^{-1} h^{-1} (applying the Q$_{10}$ rule that activity doubles with every 10 °C increase in temperature).

The active upper layer of 0.05 m is very prone to desiccation or water logging or surface effects such as physical crusting. The sensitivity to the first two factors became apparent in the preceding column test but also in the test presented here where the drop in performance during the first phase of operation was probably caused by condensation of the moisturized air in the column headspace (Figure 11). It is therefore strongly advisable to rely on at least 0.1 to 0.2 m for methane oxidation, meaning that according to Table 6 maximum landfill gas fluxes may not exceed 0.25 l m^{-2} h^{-1}. This limit will be reduced even more by the fact that at 95 % of the Proctor density for the investigated material 10.96 vol.% of air-filled pore volume will be available only under very well drained conditions. As the air capacity of the material at this degree of compaction is very low at a matric potential of 60 hPa (compare Table 1), mitigation of emissions will be close to zero under moist conditions. Conditions can be improved by vegetation rooting.

In conclusion, the investigated sandy loam is not suitable as methane oxidising cover soil at high degrees of compaction as it will not warrant a sufficient oxidation capacity.

Table 6: Estimation of maximum LFG fluxes allowing for complete oxidation of CH$_4$ at compaction of 95 % Proctor and different heights of the active layer. Calculation of CH$_4$ oxidation activity is based on a bulk density of 1.59 g/cm^3.

Air-filled pore volume (vol.%)	D_{eff} (m^2/s)	Height of active layer (m)	O$_2$ influx (mol m^{-2} h^{-1})	max LFG flux (l m^{-2} h^{-1})	max CH$_4$ flux (l m^{-2} h^{-1})	CH$_4$ oxidation activity (µg g$_{fw}^{-1}$ h^{-1})
10.96	6.72*10^{-8}	0.2	0.011	0.13	0.08	0.43
10.96	6.72*10^{-8}	0.1	0.022	0.25	0.15	1.73
10.96	6.72*10^{-8}	0.05	0.045	0.5	0.30	6.92

4.6 Estimation of preferable air-filled pore volumes for oxidation of methane at different magnitudes of landfill gas flux

Using the abovementioned linear regression for the relationship between air-filled pore volume and diffusivity, the share of air filled pore volume necessary to supply enough oxygen to oxidise all methane supplied with the landfill gas was calculated for a range of CH$_4$ fluxes (Figure 17). An active layer of 0.2 m, a bulk density of 1.4 g cm^{-3} and a CH$_4$ concentration of 60 vol.% were assumed.
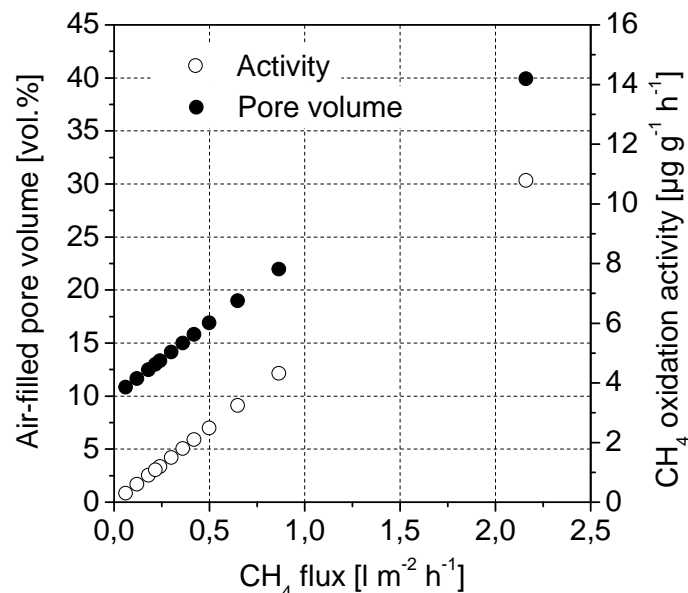

Figure 17: Share of air-filled pore volume necessary to oxidise various CH$_4$ fluxes and corresponding CH$_4$ oxidation activities. Activity refers to fresh weight.

The graph shows that under the given assumptions and the limit activity of approximately 5 µg g^{-1} h^{-1} over the year no more than 1 l CH$_4$ m^{-2} h^{-1} can be oxidised. The necessary pore volume would range around 25 vol.%. Under conditions of field capacity this would only be fulfilled by pure sands. To oxidise 0.5 l m^{-2} h^{-1}, about 17 vol.% of pore volume would be needed which would be fulfilled by lightly loamy, silty or clayey sands under medium compaction. The

effect of rooting and advective O$_2$ ingress as a result of the negative pressure generated by methane oxidation is not considered here.

5   Summary and conclusions

The main results and conclusions of the study are as follows:

- Compaction strongly affects the share of coarse pores > 10 µm in which water is not bound by capillary forces but can drain away and which are thus available for gas transport. Correspondingly, diffusivity and thus the supply of O$_2$ to the methanotrophic bacteria are strongly influenced by the degree of compaction. This was shown by the diffusion tests, which yielded a strong positive correlation between air-filled pore volume and the measured effective diffusion coefficient for O$_2$.

- As a result of the reduced diffusivity, the concentration of atmospheric components (O$_2$, N$_2$) in the columns in comparable depths and at similar influx rates decreased with increasing degree of compaction.

- In all columns, the extent of ingress of atmospheric air from above decreased with increasing inlet fluxes. At the highest degree of compaction (95 % of the Proctor density), however, air ingress fell to very low values at the second highest flux, whereas the two other columns maintained significant levels of air over the range of fluxes tested. Especially column 4 at 75 % compaction was very well aerated across the entire depth and through the entire experiment. Subsequently, CH$_4$ oxidation already occurred in the gravel gas distribution layer.

- At the lowest degree of compaction (column 4, 75 %), the limit of the oxidation capacity of the system was not reached, i.e. oxidation efficiencies were always close to 100 % at a maximum oxidation rate of 4.8 l CH$_4$ m^{-2} h^{-1}. At the highest degree of compaction (column 1, 95 %), oxidation rates were high at lower fluxes but sensitive to the prevailing conditions of moisture, so that also very low efficiencies were recorded at low inlet fluxes. The highest oxidation rate was 2.2 l CH$_4$ m^{-2} h^{-1}. The average oxidation rate dropped with increasing influx rates, partly collapsing to zero. At 85 % compaction, the oxidation rate also dropped with increasing inlet fluxes, but significantly higher levels were maintained than at 95 % compaction. The highest oxidation rate for this column was 5.3 l CH$_4$ m^{-2} h^{-1}.

- The given material, a sandy loam, compacted to 95 % of the Proctor density does not provide enough diffusivity to ascertain methane oxidation all year round as the active oxidation zone is restricted to the upper crust of the material.

6   References

Ad-Hoc-Arbeitsgruppe Boden (2005): Bodenkundliche Kartieranleitung. 5. Auflage.

FAO - ISRIC & ISSS (eds.) (2006): World reference base for soil resources 2006: a framework for international classification, correlation and communication. World soil resources reports, 103. Rome.

Gebert, J., Gröngröft, A., Miehlich, G. (2003): Kinetics of microbial landfill methane oxidation in biofilters. Waste Management 23: 609-619.

Gebert, J., Rachor, I., Gröngröft, A. (2008): Column study for assessing the suitability of different soil substrates for CH$_4$ oxidation in landfill covers. Report to melchior+wittpohl Ingenieurgesellschaft, 31 p.